NUMERICAL METHODS FOR FAST MAGNETOACOUSTIC WAVES IN SOLAR CORONAL LOOPS

MARCIN GRUSZECKI AND KRZYSZTOF MURAWSKI

Faculty of Physics, Mathematics and Informatics, UMCS,
Radziszewskiego 10, 20-031 Lublin, Poland
marcingruszecki@wp.pl, kmur@kft.umcs.lublin.pl

(Received 14 August 2008; revised manuscript received 1 December 2008)

Abstract: Numerical methods for standing fast magnetoacoustic kink waves in an isothermal solar coronal slab with a field aligned flow are considered. Such waves are triggered impulsively by a velocity pulse that is initially launched in an ambient medium. The spatial and temporal signatures of these waves are determined by solving two-dimensional, ideal magnetohydrodynamic equations numerically. The Ramses code which resolves complex spatial structures by adopting an adaptive mesh refinement technique and shock-capturing capabilities is used. The numerical results show that spatial and temporal wave signatures are reminiscent to the recent observational findings.

Keywords: numerical simulations, Godunov methods, magnetohydrodynamics

1. Introduction

The development of numerical techniques for solving an initial-value problem for magnetohydrodynamic (MHD) equations has been slower than for hydrodynamics which is due to the intrinsic complexity of these equations. As a result, most numerical schemes have been based for a long time on methods dependent on artificial viscosity to represent shocks adequately. The past experience with fully conservative, high-order upwind hydrodynamic codes have revealed them to be superior in many applications. There are two principal difficulties associated with a numerical solution of MHD equations compared to hydrodynamic equations: (a) MHD equations have new families of waves; (b) the magnetic field has to satisfy the divergence-free constraint, $\nabla \cdot \boldsymbol{B} = 0$. Despite these problems, many numerical schemes have been nevertheless developed for MHD equations.

In this paper the results of numerical simulations of MHD waves in solar coronal loops which are high-density regions of closed magnetic field structures that ubiquitously reside in the solar corona are presented. Despite a number of early reports on oscillations in coronal magnetic structures (see [1] for a review), detection of oscillations by the Transition Region and Coronal Explorer (TRACE) spacecraft [2, 3] has convincingly demonstrated the presence of oscillations in cold coronal loops. Oscillations in hot loops have also been detected by the Solar Ultraviolet Measurements of Emitted Radiation Spectrometer (SUMER) on the Solar and Heliospheric Observatory (SOHO) [4] and by the Hinode spacecraft recently [5]. The Hinode satellite observed oscillations that were seen for about 3 wave-periods, with a wave-period lasting for about 2 minutes (an average wave-period was estimated for 113 s) in a 71 Mm long loop. The oscillations occurred in the presence of a background flow whose magnitude was estimated in the range of 74–123 $\mathrm{km\,s^{-1}}$.

These recent observations of oscillatory phenomena in coronal loops have provided a significant impetus to the theoretical development of the wave theory. The theory of coronal loop oscillations has been developed by a number of authors (see [6] for a review). In particular, Gruszecki *et al.* [7] constructed a model of loop oscillations which were reported by Ofman and Wang [5]. In this model a coronal loop was approximated by a straight slab of a cold plasma with a field aligned flow which was initially set either uniform or inhomogeneous within the slab. Gruszecki *et al.* showed that the effect of such a flow was to attenuate the wave amplitude, while a wave-period was very weakly altered.

A main goal of this paper is to present numerical methods for a model which is an extension of the model of Gruszecki *et al.* [7]. An isothermal slab with an aligned flow which is implemented into the system by inflow boundary conditions is considered. As the flow can be kept constant, such a model is more realistic than the former model of Gruszecki *et al.* The plasma conditions within a photosphere-like layer have been modified, as well.

This paper is organized as follows. The numerical model is described in the following section. The numerical results are presented and discussed in Section 3. The paper is concluded by a short summary of the main results in Section 4.

2. Numerical model for MHD equations

Coronal plasma is described with using the ideal MHD equations, *viz.*:

$$\boldsymbol{q}_{,t}+\nabla\cdot\boldsymbol{f}=0,\qquad \nabla\cdot\boldsymbol{B}=0, \tag{1}$$

where:

$$\boldsymbol{q}=(\varrho,\varrho\boldsymbol{v},\boldsymbol{B},E)^T, \tag{2}$$

$$\begin{aligned}\boldsymbol{f}=\big(\varrho\boldsymbol{v},\varrho\boldsymbol{v}\boldsymbol{v}+\boldsymbol{I}(p+\frac{B^2}{2})-\boldsymbol{B}\boldsymbol{B},\boldsymbol{v}\boldsymbol{B}-\boldsymbol{B}\boldsymbol{v},\\ (E+p+\frac{B^2}{2})\boldsymbol{v}-\boldsymbol{B}(\boldsymbol{v}\cdot\boldsymbol{B})\big)^T.\end{aligned} \tag{3}$$

ϱ in the equations is the mass density, p is the gas pressure, $\boldsymbol{v}=[v_{\mathrm{x}},v_{\mathrm{y}},v_{\mathrm{z}}]$ is the flow velocity, μ is the magnetic permeability, $\gamma=5/3$ is the adiabatic index, $\boldsymbol{I}$ is the 3×3 identity matrix, $\boldsymbol{v}\boldsymbol{v}$ stands for the 3×3 tensor v_iv_j, and $\boldsymbol{B}=[B_{\mathrm{x}},B_{\mathrm{y}},B_{\mathrm{z}}]$ is normalized by the $\sqrt{\mu}$ magnetic field.

The plasma state of Equation (2) in the finite volume method is advanced in time by evaluating the fluxes of Equation (3) at the interfaces between neighboring states. In order that the Rankine-Hugoniot conditions should be satisfied at these interfaces, these fluxes must contain some kind of dissipation and a flux limiter must be applied to minimize the post-shock oscillation [8].

2.1. A plasma slab model

An equilibrium state which consists of a straight slab model with an enhanced mass density and flowing plasma over a width of a in an otherwise uniform and still medium is considered, *viz.*:

$$\varrho(z),V(z)\hat{\boldsymbol{x}},p(z),B(z)\hat{\boldsymbol{x}}=\begin{cases}\varrho_{\rm i},V_0,p_{\rm i},B_{\rm i}, & |z|\le a,\\ \varrho_{\rm e},0,p_{\rm e},B_{\rm e}, & |z|>a.\end{cases} \tag{4}$$

In this case, the magnetic field is uniform and directed along the x-direction and the slab width, a, is chosen equal to 2.5 Mm. The mass density within the slab, $\varrho_{\rm i}$, is assumed to be 5 times larger than in the ambient medium, $d=\varrho_{\rm i}/\varrho_{\rm e}=5$. This value is consistent with the observational data of Aschwanden and Nightingale [9]. Gas and magnetic pressures within the slab (index $_{\rm i}$) and in the ambient medium (index $_{\rm e}$) are chosen to satisfy the equilibrium condition:

$$p_{\rm i}+\frac{B_{\rm i}^2}{2\mu}=p_{\rm e}+\frac{B_{\rm e}^2}{2\mu}. \tag{5}$$

In particular, $p_{\rm i}/p_{\rm e}=\varrho_{\rm i}/\varrho_{\rm e}$ is chosen which gives a temperature ratio of $T_{\rm i}/T_{\rm e}=1$. Additionally, dense plasma layers are implemented at the left, right and top sides of the simulation region. This can be done by setting the mass density $\tilde{\varrho}_{\rm e}(x,z)$:

$$\begin{aligned}\tilde{\varrho}_{\rm e}(x,z)=\varrho_{\rm e}+\frac{1}{2}\varrho_{\rm e}(d_{\rm ph}-1)\Bigg\{&\left[1-\tanh\left(\frac{x-x_{\rm l}}{s_{\rm ph}}\right)\right]+\\ &\left[1-\tanh\left(-\frac{x-x_{\rm r}}{s_{\rm ph}}\right)\right]+\left[1-\tanh\left(-\frac{z-z_{\rm r}}{s_{\rm ph}}\right)\right]\Bigg\}.\end{aligned} \tag{6}$$

In this case $s_{\rm ph}=2$ Mm is the transition region width and $x_{\rm l}=0.2\,L$, $x_{\rm r}=0.91\,L$ and $z_{\rm r}=1.01\,L$ denote the left, right and top positions of the dense layers. By this choice, the left and right dense layers are separated by the distance of the slab length in the coronal medium, $L_{\rm S}=71$ Mm. The symbol $d_{\rm ph}$ denotes the ratio of the photosphere mass density to the ambient medium and the dense photosphere layers serve as natural wave reflectors. These layers mimic the photosphere action and comprise the necessary ingredients of the developed model. Initial configurations of the slab and the photosphere-like layers are shown in Figure 1. It is noteworthy that the mass density within the region $|z|\le a$ is independent of x; the slab enters the photosphere-like layers without exhibiting any mass density variation there. As a result, flowing plasma enters the left and right dense layers without any reflection.

Our discussion is limited to a two-dimensional magnetically structured medium in which all equilibrium plasma variables are invariant in the y-direction, $\partial/\partial y=0$, and the magnetic field and flow are polarized in the $x-z$ plane such that $V_{\rm y}=B_{\rm y}=0$. As a result of this assumption, the Alfvén wave is removed from the system which is able to propagate fast and slow magnetoacoustic waves only.

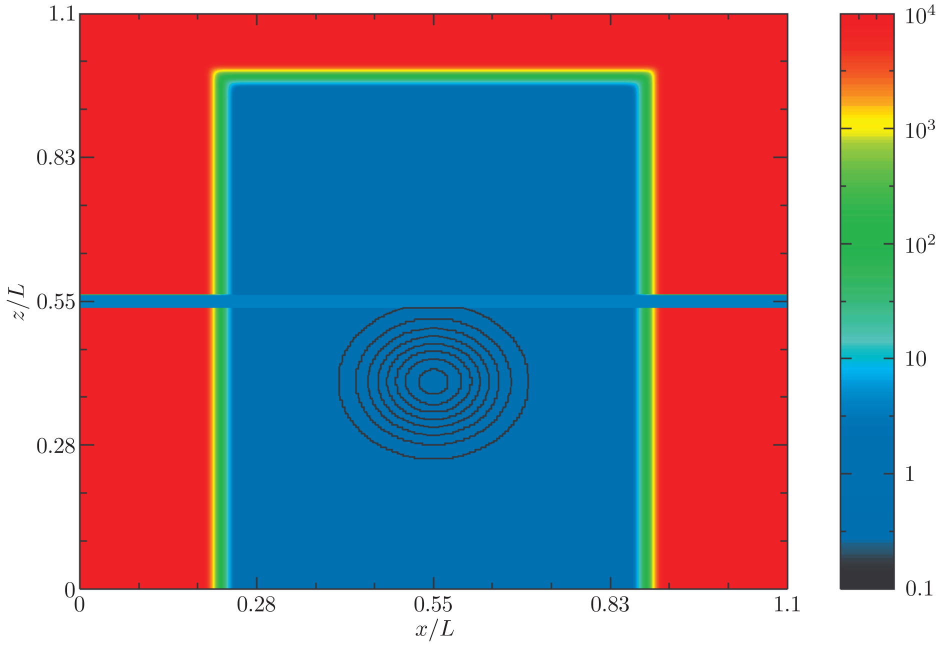

Figure 1. Equilibrium mass density profile representing a straight coronal slab. Note the dense photosphere layers for $x<0.2\,L$, $x>0.91\,L$ and $z>1.01\,L$. The contours denote the initial pulse

2.2. Perturbations

The above equilibrium state is initially (at $t=0$) perturbed by the initial Gaussian pulse in a vertical component of velocity:

$$V_z(x,z,t=0)=V_{z0}\,e^{-\left(\frac{x-L/2}{2w_x}\right)^2}e^{-\left(\frac{z-L/2}{2w_z}\right)^2}. \tag{7}$$

Such a pulse triggers fast magnetoacoustic waves which have been recently observed in a solar coronal loop by Ofman and Wang [5]. Perturbations in other plasma quantities can also be implemented but they would not change a general scenario of the excitation of fast magnetoacoustic waves. In the above formula $V_{z0}=0.2\;c_{Ae}$ denotes the initial pulse amplitude. The symbols w_x and w_z are the initial flow profile half-widths.

In this paper, Alfvén, $c_{Ae}=\sqrt{B_e/\mu\varrho_e}$, and sound, $c_{se}=\sqrt{\gamma p_e/\varrho_e}$, speeds in the ambient coronal medium are selected and held fixed as $c_{Ae}=1.13\cdot10^6$ m/s and $c_{se}=2\cdot10^5$ m/s. As a result, plasma beta in the ambient medium, $\beta_e=2\mu p_e/B_e^2=0.04$ and within the slab, $\beta_i=2\mu p_i/B_i^2=0.23$.

3. Numerical results

The Ramses code as described by Teyssier [8] and Fromang *et al.* [10] is used to obtain numerical results. Ramses is a grid based code that is developed for astrophysical plasma dynamics applications. This code implements the higher-order Godunov method, *e.g.* [11]. Numerical fluxes are computed using a linearised Riemann solver and the divergence-free condition is satisfied with the use of a constrained transport method. This code implements the adaptive mesh refinement technique to increase the spatial resolution of complex flow structures. An Eulerian box $(0,2\,L)\times(0,2\,L)$ is used to represent a physical region. This box is covered by an adaptive mesh, with a tree-based data structure, permitting recursive grid refinements on a cell-by-cell basis. A mesh consisting of 5-10 grid levels is used. Errors in mass density gradients are taken into account as a mesh refinement criterion. Inflow boundary conditions are set at the left edge of the simulation region, specifying all plasma parameters according to Equation (4). Open boundary conditions are implemented at all remnant edges of the simulation region, allowing an outgoing wave signal to leave the simulation area freely.

The momentum pulse of Equation (7) launched at $t = 0$ s above the slab triggers essentially fast magnetoacoustic waves for all the simulations. Vertical oscillations of the dense curved slab are then excited as this pulse reaches a slab location. Figure 2 shows the time-signature of these oscillations by plotting the evolution of the mass density vertical profile with time near the slab center. This time-signature reveals fast magnetoacoustic slab oscillations that slowly decay with the wave attenuation time τ.

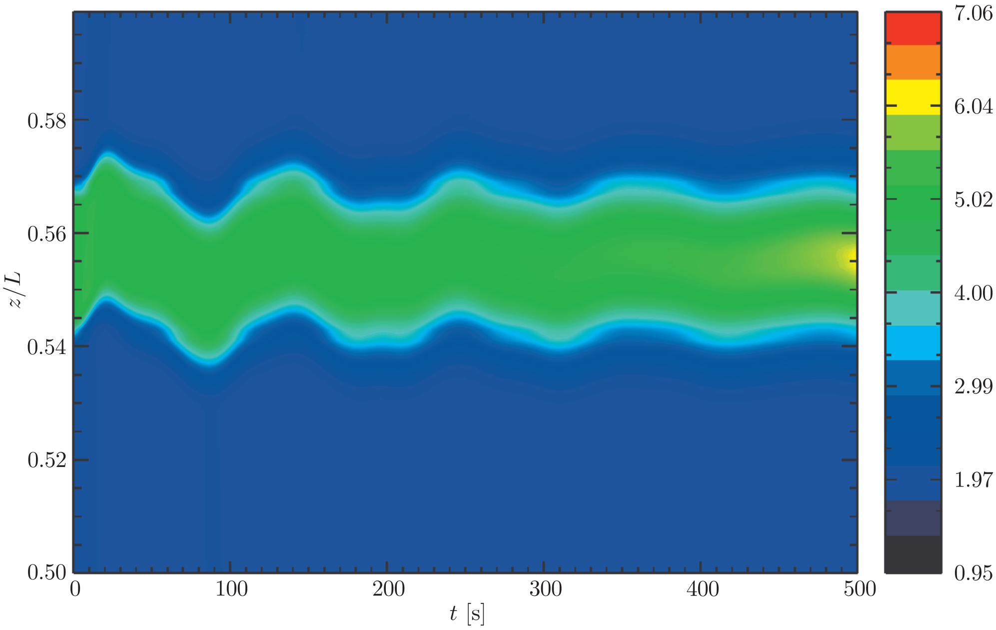

Figure 2. Time-signatures of mass density evaluated at slab center

Figure 3 presents the wave-period P as a function of the mass density contrast between the photospheric-like layer and the ambient medium, d_{ph}. It is clear that P falls off with d_{ph} which is in agreement with our expectations. The fast magentoacoustic waves for a larger value of d_{ph} penetrate the photosphere-like layers at the slab ends to a smaller extent. As a result, the effective slab length is shorter (Figure 4) and P becomes smaller. It is noteworthy that P for the fundamental kink mode:

$$P = \frac{2l}{c_{\mathrm{k}}}, \tag{8}$$

where l is the slab length and c_{k} denotes the kink speed which satisfies the condition, $V_{\mathrm{Ai}} < c_{\mathrm{k}} < V_{\mathrm{Ae}}$. The wave attenuation time τ is essentially independent of d_{ph} with a variance of about 0.1 s.

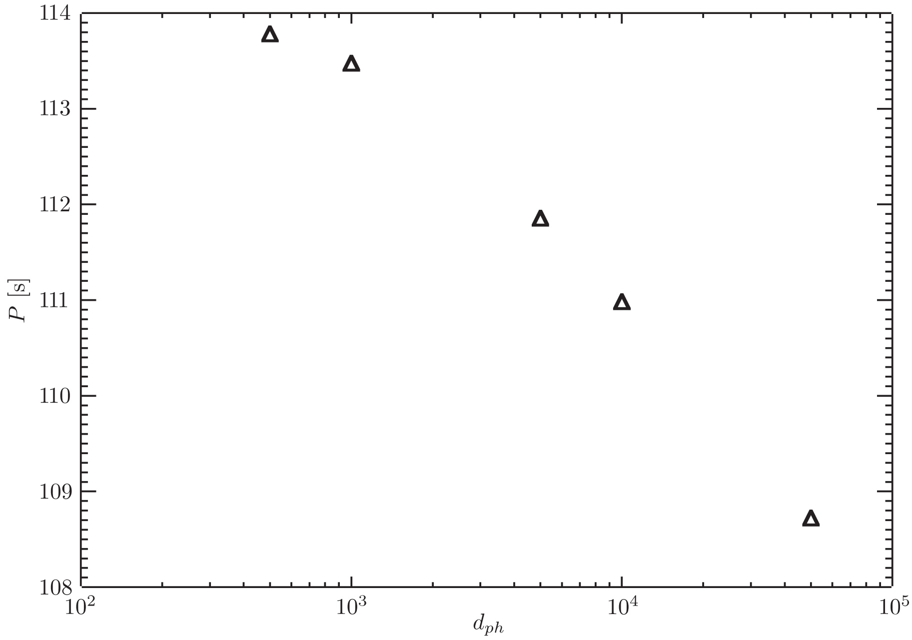

Figure 3. Wave-period P of standing fast magnetoacoutic waves vs. mass density of photosphere $d_{\rm ph}$

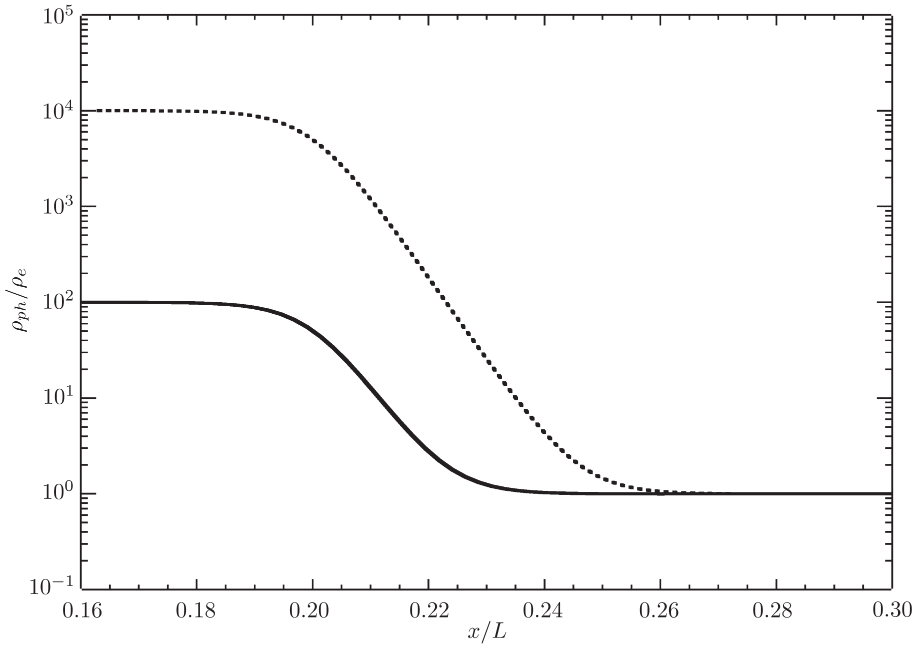

Figure 4. Horizontal mass density profiles for a 10^2 (solid line) and 10^4 (dotted line) denser photosphere than the ambient coronal medium

4. Summary

A numerical model of fast magnetoacoutic waves in a solar coronal loop that is modeled by a plasma slab has been presented in this paper. Our findings can be summarized as follows. The initial momentum pulse imposed at the start of the simulation triggers vertical slab oscillations that exhibit leakage into a photosphere-like layer [7] and into the ambient medium. The numerical results obtained in this paper are akin to the observational data of Ofman and Wang [5].

Acknowledgements

MG's and KM's work has been supported by a grant from the Polish Ministry of Science for 2007–2010.

References

[1] Aschwanden M J 1987 *Solar Phys.* **111** 113
[2] Aschwanden M J, Fletcher L, Schrijver C J and Alexander D 1999 *Astrophys. J.* **520** 880
[3] Nakariakov V M, Ofman L, Deluca E E, Roberts B and Davila J M 1999 *Science* **285** 862
[4] Wang T J, Solanki S K, Curdt W, Innes D E and Dammash I E 2002 *Astrophys. J.* **574**, L101
[5] Ofman L and Wang T J 2008 *Astron. Astrophys.* **482**, L9
[6] Nakariakov V M and Verwichte E 2005 *Living Reviews in Solar Physics* **2** 3
[7] Gruszecki M, Murawski K and Ofman L 2008 *Astron. Astrophys.* **488** 757
[8] Teyssier R 2002 *Astron. Astrophys.* **385** 337
[9] Aschwanden M J and Nightingale R W 2005 *Astrophys. J.* **633** 499
[10] Fromang S, Hennebelle P and Teyssier R 2006 *Astron. Astrophys.* **457** 371
[11] Murawski K 2002 *Analytical and Numerical Methods for Wave Propagation in Fluids*, World Scientific, Singapore